

# Reduced arsenic clearance and increased toxicity in aquaglyceroporin-9-null mice

Jennifer M. Carbrey<sup>a,1</sup>, Linhua Song<sup>a</sup>, Yao Zhou<sup>b,c</sup>, Masafumi Yoshinaga<sup>c,d</sup>, Aleksandra Rojek<sup>e</sup>, Yiding Wang<sup>a</sup>, Yangjian Liu<sup>a</sup>, Heidi L. Lujan<sup>f</sup>, Stephen E. DiCarlo<sup>f</sup>, Søren Nielsen<sup>e</sup>, Barry P. Rosen<sup>c,d</sup>, Peter Agre<sup>a,g,1</sup>, and Rita Mukhopadhyay<sup>b,c,1</sup>

<sup>a</sup>Department of Cell Biology, Duke University School of Medicine, Durham, NC 27710; Departments of <sup>b</sup>Molecular Microbiology and Infectious Disease and <sup>c</sup>Cellular Biology and Pharmacology, Florida International University College of Medicine, Miami, FL 33199; Departments of <sup>d</sup>Biochemistry and Molecular Biology and <sup>e</sup>Physiology, Wayne State University School of Medicine, Detroit, MI 48201; <sup>f</sup>Water and Salt Research Center, University of Aarhus, Aarhus DK-8000, Denmark; and <sup>g</sup>Department of Molecular Microbiology and Immunology and Malaria Research Institute, The Johns Hopkins Bloomberg School of Public Health, Baltimore, MD 21205

Contributed by Peter Agre, July 29, 2009 (sent for review June 20, 2009)

**Expressed in liver, aquaglyceroporin-9 (AQP9) is permeated by glycerol, arsenite, and other small, neutral solutes. To evaluate a possible protective role, AQP9-null mice were evaluated for in vivo arsenic toxicity. After injection with NaAsO<sub>2</sub>, AQP9-null mice suffer reduced survival rates (LD<sub>50</sub>, 12 mg/kg) compared with WT mice (LD<sub>50</sub>, 15 mg/kg). The highest tissue level of arsenic is in heart, with AQP9-null mice accumulating 10–20 times more arsenic than WT mice. Within hours after NaAsO<sub>2</sub> injection, AQP9-null mice sustain profound bradycardia, despite normal serum electrolytes. Increased arsenic levels are also present in liver, lung, spleen, and testis of AQP9-null mice. Arsenic levels in the feces and urine of AQP9-null mice are only ≈10% of the WT levels, and reduced clearance of multiple arsenic species by the AQP9-null mice suggests that AQP9 is involved in the export of multiple forms of arsenic. Immunohistochemical staining of liver sections revealed that AQP9 is most abundant in basolateral membrane of hepatocytes adjacent to the sinusoids. AQP9 is not detected in heart or kidney by PCR or immunohistochemistry. We propose that AQP9 provides a route for excretion of arsenic by the liver, thereby providing partial protection of the whole animal from arsenic toxicity.**

Evolutionary exposure to environmental arsenic has led to selection of organisms ranging from microbes to mammals with mechanisms for coping with arsenic toxicity. Humans may be inadvertently exposed to arsenic from water contaminated from geological sources or industrial pollution. Up to 57 million people in Bangladesh presently drink groundwater with arsenic concentrations above the World Health Organization acceptable standard (1). In clinical medicine, arsenic trioxide is used in tandem with *all-trans*-retinoic acid to treat acute promyelocytic leukemia (2, 3), and drugs containing arsenic and antimony are used to treat parasitic infections, African sleeping sickness, and leishmaniasis (4).

Transport proteins are critical in the response to arsenic toxicity, because uptake and export are two key features in the cellular drug response. Members of the ATP-binding cassette transporter family export certain drugs, and some cell lines resistant to arsenic have increased expression of multidrug-resistance proteins (MRPs) (5–7). MRP1-null mice exhibit increased sensitivity to sodium arsenite (8). Multidrug-resistance gene MDR1a/1b double-null mice are even more sensitive and accumulate arsenic in their organs after exposure (9).

Several lines of evidence indicate that aquaglyceroporins are involved in arsenite uptake by mammalian cells. A member of the aquaporin gene family, yeast glycerol transporter (Fps1p), was shown to facilitate arsenite [As(III)] and antimonite [Sb(III)] uptake by eukaryotic cells (10). The mammalian aquaglyceroporins AQP3, AQP7, and AQP9 were shown to transport arsenite and antimonite (7, 11). Studies of multiple cultured cell lines revealed increased AQP3 or AQP9 expression, resulting in increased arsenic accumulation and toxicity (7, 12–15). A human

lung adenocarcinoma cell line resistant to arsenic was found to have decreased levels of AQP3 (7). When AQP3 expression was reduced further, arsenite uptake declined still further, and cellular resistance to arsenic toxicity increased (7).

Known to transport a range of small, neutral solutes (16), including arsenite, antimonite, and methylarsonous acid [MAs(III)] (11, 17), AQP9 is expressed in liver, testes, brain, and leukocytes (16, 18, 19), some tissues being sensitive to arsenite. In vivo studies may be complicated by conversion of arsenite to other forms by oxidation, reduction (20), methylation (21, 22), and glutathionylation (20, 23). Despite plentiful evidence that aquaglyceroporins are involved in arsenite transport, arsenic toxicity has not been reported in AQP9-null mice.

Here, we describe arsenic toxicity studies of AQP9-null mice compared with WT mice. We determined that AQP9-null mice suffer reduced survival after injection with sodium arsenite (NaAsO<sub>2</sub>). Increased accumulation of arsenic was observed in multiple organs of AQP9-null mice, with highest levels of arsenic in heart, accompanied by profound bradycardia. Excretion of arsenic in urine and feces of AQP9-null mice is greatly reduced. Although AQP9 is known to facilitate uptake of arsenite by single cells in culture (12–15), our studies cause us to propose that AQP9 also facilitates in vivo arsenic excretion by the liver, thereby providing partial protection against arsenic toxicity.

## Results

**Lethal Arsenic Dose.** AQP9-null mice and WT mice were s.c. injected with various doses of NaAsO<sub>2</sub> to determine the median lethal dose. At doses of NaAsO<sub>2</sub> of 12, 13, and 15 mg/kg, AQP9-null mice suffered lower survival rates than the WT mice (Fig. 1). The LD<sub>50</sub> for the AQP9-null mice was 12 mg/kg, compared with 15 mg/kg for the WT mice.

**Organ Accumulation of Arsenic.** AQP9-null mice and WT mice received injections into the peritoneum with 10 mg/kg NaAsO<sub>2</sub>. After 12–24 h, organs were harvested to determine the arsenic concentration by inductively coupled plasma mass spectrometry (ICP-MS). In most organs tested, AQP9-null mice had much higher concentrations of arsenic compared with WT mice. The highest accumulation was in AQP9-null heart, at ≈10–20 times the arsenic level found in WT hearts (Fig. 2). Arsenic levels were comparably high in bladder of both AQP9-null mice and WT mice. Although lower than heart, arsenic levels were measured in liver, lung, spleen, and testis, with the AQP9-null levels

Author contributions: J.M.C., P.A., and R.M. designed research; J.M.C., L.S., Y.Z., M.Y., A.R., Y.W., Y.L., H.L.L., S.E.D., and R.M. performed research; J.M.C., A.R., S.E.D., S.N., B.P.R., P.A., and R.M. analyzed data; and J.M.C. and P.A. wrote the paper.

The authors declare no conflict of interest.

<sup>1</sup>To whom correspondence may be addressed. E-mail: jennifer.carbrey@duke.edu, pagre@jhsp.edu, or rmukhop@fiu.edu.



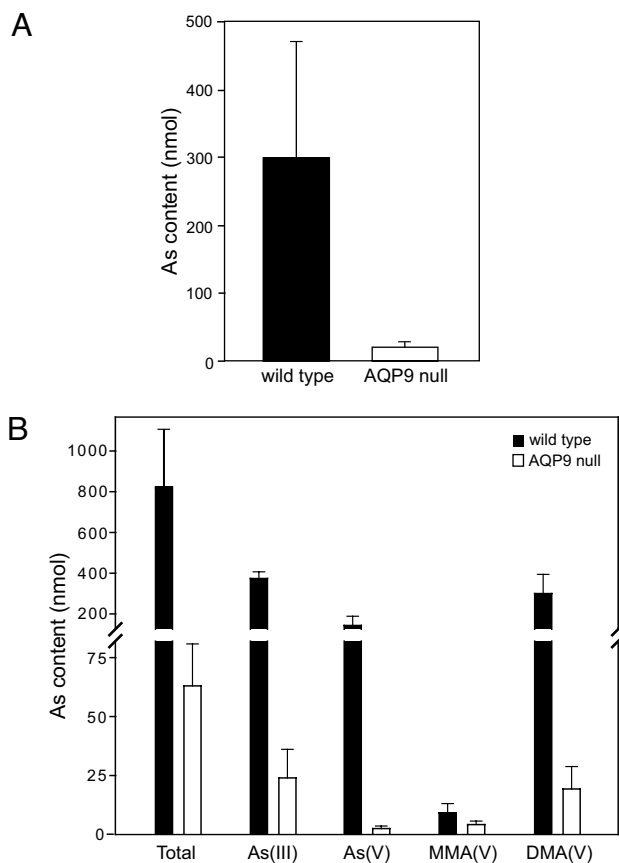


**Fig. 4.** Arsenic excretion in feces and urine in WT and AQP9-null mice. (A) Arsenic content of feces from five WT and five AQP9-null mice 24 h after 10 mg/kg NaAsO<sub>2</sub> injection. (B) Arsenic content and speciation in the urine of four WT and four AQP9-null mice 24 h after 10 mg/kg NaAsO<sub>2</sub> injection. Total arsenic content of urine from WT and AQP9-null mice and the amount of the various arsenic species in the urine are shown. Error bars represent SEM.

those mice. To confirm this, AQP9-null mice and WT mice were injected i.p. with 10 mg/kg NaAsO<sub>2</sub>. After injection, mice were kept in metabolic cages to collect urine and feces from individual animals. The amount of arsenic in feces of WT mice was more than 10-fold greater than for AQP9-null mice when measured between 12 and 24 h after injection (Fig. 4A). Similarly, the urine of WT mice contained more arsenic compared with AQP9-null mice when measured between 12 and 24 h after injection (Fig. 4B). WT mice were found to have elevated levels of arsenite [As(III)], arsenate [As(V)], and dimethylarsenate [DMA(V)] in urine compared with AQP9-null animals. In contrast, only low levels of monomethylarsenate [MMA(V)] were detected in urine of AQP9-null or WT animals (Fig. 4B).

**AQP9 Immunohistochemistry.** As reported previously, AQP9 expression is abundant in liver (16, 18), where it is specifically present in hepatocytes (16, 24). We confirmed this distribution in WT mice but not AQP9-null mice (Fig. 5A and B). Moreover, expression was most dramatic at the basolateral membranes adjacent to sinusoids. A smaller level of AQP9 expression was noted at the apical membranes where hepatocytes abut each other (Fig. 5A). This location is entirely consistent with AQP9 playing a role in the excretion of arsenic into bile; hence, the high fecal level of arsenic in the WT mice.

Possible presence of AQP9 in heart was evaluated. This was deemed important because of the pronounced level of arsenic in hearts of AQP9-null mice (Fig. 2). Moreover, the accompanying

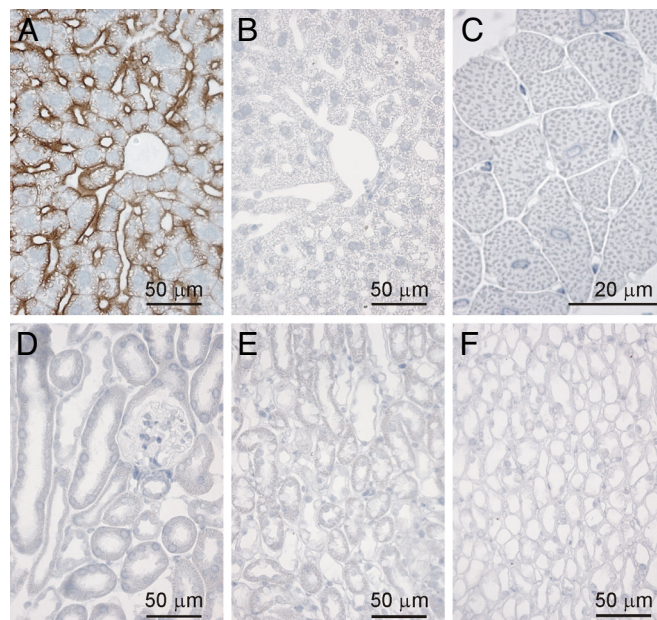


**Fig. 5.** Immunohistochemistry of tissues from WT and AQP9KO mice stained with antibody against AQP9 (RA2674-685). All tissues were stained with the same dilution of the antibody. (A) WT mouse liver showing strong staining of AQP9 in the basolateral membranes of the hepatocytes facing the liver sinusoids. (B) AQP9-KO mouse liver showing the absence of staining for AQP9. (C) WT mouse cardiac muscle showing the absence of staining for AQP9. (D–F) WT mouse kidney, showing the absence of staining for AQP9: (D) kidney cortex, (E) kidney outer medulla, and (F) kidney inner medulla.

bradycardia found in AQP9-null mice was not found in WT mice (Fig. 3). No immunohistochemical evidence for AQP9 expression was found in WT heart (Fig. 5C), suggesting that arsenic deposition and cardiotoxicity simply reflect the efficient exchange of arsenic from blood to heart. Thus, no evidence suggests that AQP9 provides an escape route for arsenic from heart.

Potential presence of AQP9 in kidney was also evaluated. This was deemed important because both AQP9-null and WT mice have high levels of arsenic in bladder (Fig. 2), and AQP9-null mice exhibit lower levels of arsenic in urine (Fig. 4B). No immunohistochemical evidence for AQP9 expression was found in kidney, including cortex, outer medulla, and inner medulla (Fig. 5D–F). Thus, the high levels of arsenic in urine of WT mice may simply result from glomerular filtration.

## Discussion

The aquaporin and aquaglyceroporin family of membrane channels have previously been implicated in multiple clinical situations, including Colton blood group incompatibility, spinal fluid dynamics, aqueous humor pressures, nephrogenic diabetes insipidus, congenital cataracts, skin hydration, brain edema, neuromyelitis optica, deafness, salivary and lacrimal gland dysfunction, fat metabolism, and malaria (reviewed in ref. 25). The studies reported here extend this impressive list to include arsenic toxicity, an important clinical disorder affecting millions of individuals in Bangladesh and other developing countries (1).

Despite impressive levels of arsenic in multiple tissues after injection of AQP9-null mice, the LD<sub>50</sub> was altered significantly but not dramatically (Fig. 1). This is not surprising, because evidence for arsenic transport by MRPs has been reported (9). Despite being measured at different institutions under somewhat different conditions, the magnitude of the differences in LD<sub>50</sub> is reasonably consistent: AQP9-null 12 mg/kg vs. WT 15 mg/kg

(Fig. 1) compared with *mdr1a/1b* double-null 14.5 mg/kg vs. WT 17 mg/kg (9). The existence of multiple arsenic transport proteins should not be surprising given the high toxicity of the arsenic, and the identification of still additional classes of arsenic transport proteins should be sought.

The decrease in LD<sub>50</sub> in the AQP9-null mice can be explained by the retention of arsenic in several organs. Some of the organs in which arsenic is accumulated are known to express AQP9, including brain, liver, lung, spleen, red blood cells, and testis (16, 18, 19, 26, 27). The organ with the highest arsenic concentration in the AQP9-null mice was heart, with ≈10-fold higher arsenic concentration than heart of WT mice. AQP9 has not been reported to be expressed in the myocardium. Our studies failed to identify AQP9 in heart by immunohistochemistry (Fig. 5C).

In response to the significant accumulation of arsenic in the heart, we monitored the WT and AQP9-null mice for arrhythmia after arsenite injection. The electrocardiograms of the AQP9-null mice revealed arrhythmia that started within 5 h after injection and lasted until at least 24 h after injection. However, serum concentrations of ions critical for heart conduction were normal in the AQP9-null mice, suggesting that arsenic is directly toxic to myocardium. It is notable that similar atrioventricular block has been observed in human patients treated with arsenic trioxide (28, 29). In addition, the duration of action potentials was prolonged in guinea pig papillary muscles (30) and cultured cardiomyocytes (31) after exposure to arsenic trioxide.

Increased accumulation of arsenic in the organs of the AQP9-null mice suggests a reduced rate of clearance and excretion from the body. We collected feces and urine from WT and AQP9-null mice 12–24 h after arsenite injection. The urine and feces from the AQP9-null mice contained only ≈10% of the arsenic levels found in feces and urine of WT mice (Fig. 4). Because arsenite is converted into many different species in the body, we analyzed the urine to determine the content of different species of arsenic in the urine. Increased concentrations of As(III), As(V), and DMA(V) were excreted in the urine by the WT mice compared with the AQP9-null mice. The reduced excretion of most of the arsenic species suggests that AQP9 may be responsible for export of multiple arsenic species. AQP9 has been shown to transport As(III) and MMA(III), which is rapidly oxidized to DMA(V) (11, 17). However, further experiments are needed to determine the species that AQP9 transports *in vivo*. In addition, injecting mice with other species of arsenic, such as As(V), may also help to determine the precise role of AQP9 in arsenic clearance.

Our results are consistent with a role for AQP9 in arsenite export, which is in contrast to previous studies of cultured cells (7, 12–15). However, our studies do not exclude a role for AQP9 in arsenite import. Further experiments at earlier time points are needed to determine whether AQP9 is involved in arsenite import in mice. In addition, there is conversion of arsenite to multiple species in mice, some of which may be exported by AQP9. Export of methylated or trivalent inorganic arsenic species by AQP9 has not been studied in cultured cells.

Provision of pure drinking water should be considered a basic human right, but this right is lacking in some of the most impoverished regions of the world. We reported previously that expression of AQP9 in liver is profoundly up-regulated by fasting experimental animals (24). However, the identities of all of the molecular determinants of AQP9 expression remain undefined. This raises a possibility that identities of small molecules that increase AQP9 expression or decrease AQP9 degradation may be discovered. It may be that pharmacological resistance to arsenic toxicity by increasing arsenic excretion could be beneficial to individuals consuming arsenic-tainted water. Thus, we feel that the studies reported here may be highly relevant in light of the continued exposure of humans to groundwater tainted with arsenic as well as the use of arsenic-containing compounds as therapeutic drugs. Certainly, more research is warranted.

## Materials and Methods

**Animals.** AQP9-null mice were generated (32) and backcrossed onto a C57BL/6 background. Genotyping was carried out by using PCR (32). Under normal physiological conditions, AQP9-null mice have an increase in blood concentrations of glycerol and triglycerides compared with WT mice (32). All experiments with mice were approved by the Duke University or Wayne State University Institutional Animal Care and Use Committees. Mice used for all experiments were 2–9 months old and were age- and sex-matched.

**LD<sub>50</sub> Studies.** WT and AQP9-null mice were *s.c.* injected with various doses of sterile NaAsO<sub>2</sub> (Sigma–Aldrich) in PBS. At least six mice were injected for each dose. Mice exhibiting neurological problems, difficulty breathing, or impaired ambulation were euthanized.

**Arsenic Accumulation in Organs.** WT and AQP9-null mice were *i.p.* injected with sterile NaAsO<sub>2</sub> (10 mg/kg) in PBS. Between 12 and 24 h after injection, different organs were harvested and digested with 70% nitric acid (0.4–0.6 g/mL) at 70 °C for 2 h. Blood was treated with 0.5 mg/mL heparin. Plasma and RBCs were digested with equal volumes of 70% nitric acid at 70 °C for 2 h. The nitric acid digests were vortexed thoroughly and centrifuged at 16,000 × *g* for 5 min at room temperature. The supernatant was diluted to a final concentration of 2% nitric acid with HPLC-grade water, and total arsenic content of each sample was determined by ICP-MS (Elan 9000; Perkin–Elmer) as described previously (33).

**ECG Recording of Mice.** ECG recording electrodes were surgically attached to six WT male mice and five AQP9-null male mice. Recording electrodes were sutured *s.c.* in a modified lead II configuration by placing the negative electrode slightly to the right of the manubrium and the positive electrode at the anterior axillary line along the fifth intercostal space on the left side. The ground electrode was sutured *s.c.* on the dorsal thorax. The electrodes were exteriorized and secured at the back of the neck. During the recovery period, the mice were handled, weighed, and acclimatized to the laboratory and investigators. The electrodes were connected to a high-impedance probe (HIP 511GA; Grass Instruments) and differential preamplifier (Grass P511; Grass Instruments). The conscious, unrestrained mice were studied in their home cages and allowed to adapt to the laboratory environment for approximately 1 h to ensure stable hemodynamic conditions. After the stabilization period, beat-by-beat ECG was recorded continuously at 4 kHz for approximately 1 h. After 1 h of recording, all mice were *i.p.* injected with sodium arsenite (10 mg/kg), and recordings continued for an additional 24 h.

The ECGs were analyzed offline to measure the R–R interval (measured from the peak of one R wave to the peak of the next R wave), the P–R interval (measured from the beginning of the P wave to the beginning of the QRS complex), QRS duration (measured from the beginning of the Q wave to the end of the S wave), and the QT interval (measured from the beginning of the QRS complex to the end of the T wave) by using the ECG analysis software, Chart (ADInstruments). A two-factor ANOVA was used to compare RR, PR, and QT intervals as well as QRS duration in WT and AQP9-null mice. The Tukey method was used as the post hoc analysis for within-group and within-condition pairwise comparisons when significant group × condition interactions were present.

To determine serum ion concentrations after NaAsO<sub>2</sub> injection, four WT and four AQP9-null mice were injected *i.p.* with a 10-mg/kg dose, and blood was collected after 24 h. Frozen serum was sent for blood chemistry analysis (Rabbit & Rodent Diagnostic Associates).

**Arsenic Excretion.** WT and AQP9-null mice were *i.p.* injected with 10 mg/kg NaAsO<sub>2</sub> and placed into individual metabolic cages (Lab Products). Feces was collected between 12 and 24 h after injection, weighed, and diluted to 4 μL/mg by using 70% nitric acid. The samples were incubated at 70 °C for 1 h, spun down to remove particulate matter, and used for ICP-MS as described above.

Urine was collected between 12 and 24 h after injection, spun to remove particulate matter, and used for HPLC and ICP-MS to determine arsenic speciation. Protein was removed from the samples by centrifugation using a 10-kDa-cutoff Amicon Ultrafilter (Millipore). The filtrate was analyzed by HPLC (Series 2000; Perkin–Elmer) and ICP-MS (ELAN 9000; Perkin–Elmer) using a reverse-phase C18 column (Jupiter 300; Jupiter) and was eluted isocratically with a mobile phase consisting of 3 mM malonic acid, 5 mM tetrabutylammonium hydroxide, and 5% methanol, pH 5.6, with a flow rate of 1.0 mL/min (34).

For total arsenic determinations, an equal volume of 70% nitric acid was added to the urine samples and incubated at 70 °C for 2 h. Debris was removed by centrifugation at 16,000 × *g* for 5 min at room temperature and processed as above for ICP-MS.

**Immunohistochemistry.** The organs of WT and AQP9-null mice were fixed by perfusion via the heart with 3% paraformaldehyde in PBS buffer (pH 7.4), postfixed for 1 h in the same fixative, and embedded in paraffin after dehydration. The tissues were cut 2  $\mu$ m thick on a rotary microtome (Leica). The sections were dewaxed with xylene and rehydrated with graded ethanol. Endogenous peroxidase activity was blocked with 0.5% H<sub>2</sub>O<sub>2</sub> in absolute methanol for 10 min. The sections were boiled for 10 min in a microwave oven in target retrieval solution (1 mM Tris, pH 9.0; and 0.5 mM EGTA). Nonspecific binding was blocked with 50 mM NH<sub>4</sub>Cl in PBS for 30 min, followed by 3  $\times$  10-min washes with PBS blocking buffer (1% BSA, 0.05% saponin, and 0.2% gelatin). The sections were incubated with primary antibody RA2674-685 (19) diluted in PBS with 0.1% BSA and 0.3% Triton X-100 overnight at 4 °C. The

sections were washed 3  $\times$  10 min with PBS wash buffer (0.1% BSA, 0.05% saponin, and 0.2% gelatin) and incubated with an HRP-conjugated secondary antibody for 1 h at room temperature. After 3  $\times$  10-min rinses with PBS wash buffer, the sites of antibody-antigen reaction were visualized with a brown chromogen produced within 10 min by incubation with 0.05% 3,3'-diaminobenzidine tetrachloride (Kem-en-Tek) dissolved in 0.1% H<sub>2</sub>O<sub>2</sub>. The sections were counterstained with Mayer's hematoxylin, dehydrated, and mounted with hydrophobic medium (Eukitt; Kindler). Light microscopy was carried out with a Leica DMRE (Leica Microsystems).

**ACKNOWLEDGMENTS.** This work was supported in part by National Institutes of Health Grants HL48268 and DK065098 (to P.A.) and AI58170 (to R.M.).

1. Kinniburgh DG, Smedley PL (2001) *Arsenic Contamination of Groundwater in Bangladesh* (British Geological Survey, Keyworth, UK), pp 231–255.
2. Tallman MS (2008) The expanding role of arsenic in acute promyelocytic leukemia. *Semin Hematol* 45:525–529.
3. Hu J, et al. (2009) Long-term efficacy and safety of *all-trans* retinoic acid/arsenic trioxide-based therapy in newly diagnosed acute promyelocytic leukemia. *Proc Natl Acad Sci USA* 106:3342–3347.
4. Borst P, Ouellette M (1995) New mechanisms of drug resistance in parasitic protozoa. *Annu Rev Microbiol* 49:427–460.
5. Huang RN, Lee TC (1996) Arsenite efflux is inhibited by verapamil, cyclosporin A, and GSH-depleting agents in arsenite-resistant Chinese hamster ovary cells. *Toxicol Appl Pharmacol* 141:17–22.
6. Vernhet L, Allain N, Bardiau C, Anger JP, Fardel O (2000) Differential sensitivities of MRP1-overexpressing lung tumor cells to cytotoxic metals. *Toxicology* 142:127–134.
7. Lee TC, Ho IC, Lu WJ, Huang JD (2006) Enhanced expression of multidrug resistance-associated protein 2 and reduced expression of aquaglyceroporin 3 in an arsenite-resistant human cell line. *J Biol Chem* 281:18401–18407.
8. Lorico A, et al. (1997) Disruption of the murine MRP (multidrug resistance protein) gene leads to increased sensitivity to etoposide (VP-16) and increased levels of glutathione. *Cancer Res* 57:5238–5242.
9. Liu J, Liu Y, Powell DA, Waalkes MP, Klaassen CD (2002) Multidrug-resistance mdr1a/1b double knockout mice are more sensitive than wild type mice to acute arsenic toxicity, with higher arsenic accumulation in tissues. *Toxicology* 170:55–62.
10. Wysocki R, et al. (2001) The glycerol channel Fps1p mediates the uptake of arsenite and antimonite in *Saccharomyces cerevisiae*. *Mol Microbiol* 40:1391–1401.
11. Liu Z, et al. (2002) Arsenite transport by mammalian aquaglyceroporins AQP7 and AQP9. *Proc Natl Acad Sci USA* 99:6053–6058.
12. Bhattacharjee H, Carbrey J, Rosen BP, Mukhopadhyay R (2004) Drug uptake and pharmacological modulation of drug sensitivity in leukemia by AQP9. *Biochem Biophys Res Commun* 322:836–841.
13. Leung J, Pang A, Yuen WH, Kwong YL, Tse EW (2007) Relationship of expression of aquaglyceroporin 9 with arsenic uptake and sensitivity in leukemia cells. *Blood* 109:740–746.
14. Miao ZF, et al. (2009) Increased aquaglyceroporin 9 expression disrupts arsenic resistance in human lung cancer cells. *Toxicol In Vitro* 23:209–216.
15. Shinkai Y, Sumi D, Toyama T, Kaji T, Kumagai Y (2009) Role of aquaporin 9 in cellular accumulation of arsenic and its cytotoxicity in primary mouse hepatocytes. *Toxicol Appl Pharmacol* 237:232–236.
16. Tsukaguchi H, et al. (1998) Molecular characterization of a broad selectivity neutral solute channel. *J Biol Chem* 273:24737–24743.
17. Liu Z, Styblo M, Rosen BP (2006) Methylarsonous acid transport by aquaglyceroporins. *Environ Health Perspect* 114:527–531.
18. Ishibashi K, et al. (1998) Cloning and functional expression of a new aquaporin (AQP9) abundantly expressed in the peripheral leukocytes permeable to water and urea, but not to glycerol. *Biochem Biophys Res Commun* 244:268–274.
19. Elkjaer M, et al. (2000) Immunolocalization of AQP9 in liver, epididymis, testis, spleen, and brain. *Biochem Biophys Res Commun* 276:1118–1128.
20. Winski SL, Carter DE (1995) Interactions of rat red blood cell sulfhydryls with arsenate and arsenite. *J Toxicol Environ Health* 46:379–397.
21. Creclius EA (1977) Changes in the chemical speciation of arsenic following ingestion by man. *Environ Health Perspect* 19:147–150.
22. Lerman S, Clarkson TW (1983) The metabolism of arsenite and arsenate by the rat. *Fundam Appl Toxicol* 3:309–314.
23. Kala SV, et al. (2000) The MRP2/cMOAT transporter and arsenic-glutathione complex formation are required for biliary excretion of arsenic. *J Biol Chem* 275:33404–33408.
24. Carbrey JM, et al. (2003) Aquaglyceroporin AQP9: Solute permeation and metabolic control of expression in liver. *Proc Natl Acad Sci USA* 100:2945–2950.
25. Carbrey JM, Agre P (2009) Discovery of the aquaporins and development of the field. *Handb Exp Pharmacol* 190:23–28.
26. Liu Y, et al. (2007) Aquaporin 9 is the major pathway for glycerol uptake by mouse erythrocytes, with implications for malarial virulence. *Proc Natl Acad Sci USA* 104:12560–12564.
27. Li C, et al. (2005) Distribution of aquaporin-9 in the rat: An immunohistochemical study. *Int J Tissue React* 27:51–58.
28. Shen ZX, et al. (1997) Use of arsenic trioxide (As<sub>2</sub>O<sub>3</sub>) in the treatment of acute promyelocytic leukemia (APL): II. Clinical efficacy and pharmacokinetics in relapsed patients. *Blood* 89:3354–3360.
29. Huang SY, et al. (1998) Acute and chronic arsenic poisoning associated with treatment of acute promyelocytic leukaemia. *Br J Haematol* 103:1092–1095.
30. Chiang CE, Luk HN, Wang TM, Ding PY (2002) Prolongation of cardiac repolarization by arsenic trioxide. *Blood* 100:2249–2252.
31. Ficker E, et al. (2004) Mechanisms of arsenic-induced prolongation of cardiac repolarization. *Mol Pharmacol* 66:33–44.
32. Rojek AM, et al. (2007) Defective glycerol metabolism in aquaporin 9 (AQP9) knockout mice. *Proc Natl Acad Sci USA* 104:3609–3614.
33. Figarella K, et al. (2007) Biochemical characterization of *Leishmania major* aquaglyceroporin LmAQP1: Possible role in volume regulation and osmotaxis. *Mol Microbiol* 65:1006–1017.
34. Cui X, Kobayashi Y, Hayakawa T, Hirano S (2004) Arsenic speciation in bile and urine following oral and intravenous exposure to inorganic and organic arsenicals in rats. *Toxicol Sci* 82:478–487.